

Multi-TeV flaring from blazars: Markarian 421 a case study

Sarira Sahu*, Luis Salvador Miranda*, Subhash Rajpoot†

**Instituto de Ciencias Nucleares, Universidad Nacional Autónoma de México,
Circuito Exterior, C.U., A. Postal 70-543, 04510 Mexico DF, Mexico*

†*Department of Physics & Astronomy, California State University,
1250 Bellflower Boulevard, Long Beach, CA, 90840, USA*

The TeV blazar Markarian 421 underwent multi-TeV flaring during April 2004 and simultaneously observed in x-ray and TeV energies. It was observed that the TeV outbursts had no counterparts in the lower energies, which implies that this might be an orphan flare. In the context of hadronic model, we have shown that this multi-TeV flaring can be produced due to the interaction of Fermi-accelerated protons of energy $\lesssim 168$ TeV with the background photons in the low energy tail of the synchrotron self-Compton spectrum of the blazar jet. We fit very well the flaring spectrum with this model. Based on this study, we speculate that Mrk 501 and PG 1553+113 are possible candidates for orphan flaring in the future.

PACS numbers: 14.60.Pq; 14.60.St; 95.85.Ry

I. INTRODUCTION

Active galactic nuclei (AGN) emit electromagnetic radiation from radio to gamma-rays and exhibit large luminosity variations on time scales ranging from less than an hour up to several years. A super massive black hole is believed to sit at the center of the AGN surrounded by an accretion disk in the inner region and a torus of gas cloud in the outer region. Oppositely directed relativistic jets are ejected from the AGN which are perpendicular to the accretion disk and the torus. In the framework of the unification scheme of AGN, blazars and radio galaxies are intrinsically the same objects viewed at different angles with respect to the jet axis. When the angle between the jet and the line of sight is small it is called blazar and in contrast, for radio galaxies, the angle between the jet and the light of sight is large. Almost all AGN detected at very high energy (VHE) (> 100 GeV) are blazars with the exception of the three objects, Centaurus A (Cen A)[1, 2], M87 and NGC 1275 which are radio galaxies[3, 4]. The spectral energy distribution (SED) of these AGN have a double peak structure (in $\nu - \nu F_\nu$ plane). The low energy peak corresponds to the synchrotron radiation from a population of relativistic electrons in the jet. Although the general consensus is that the high energy peak corresponds to the synchrotron self Compton (SSC) scattering of the high energy electrons with their self-produced synchrotron photons, this result remains inconclusive for various reasons. However, this model is very successful in explaining the multi wavelength emission from blazars and FR I galaxies[1–4].

Although the SSC model seems to work very well to explain the SED of AGN up to the second peak [5, 6], difficulties arise in explaining the multi-TeV emission detected in Cen A[7], flares from the radio galaxy M87 [8], the flares from blazars 1ES 1959+650[9, 10] and Markarian 421 (Mrk 421)[11]. Also the inevitable outcome of the leptonic scenario is that, emission in multi-TeV energy has to be accompanied by a simultaneous enhanced emission in synchrotron peak. Unfortunately the enhanced

synchrotron emission was not observed in the flaring of 1ES 1959+650 in June 2002[9] and also probably in the flaring of Mrk 421 in April 2004[11], which implies that SSC model may not be efficient enough to contribute in the multi-TeV regime. On the other hand, in the hadronic models, the high energy peak (multi-TeV) is produced by the proton synchrotron emission or decay of neutral pions which are produced due to proton-proton (pp) or proton-photon (p γ) interactions. It was shown earlier that normally the pp process is inefficient to produce γ -rays in the blazar environment unless the jet-cloud interaction is taken into consideration[12–14].

II. PHOTOHADRONIC MODEL

To address the multi-TeV emission from Cen A, M87 and the orphan flaring from 1ES 1959+650, Sahu et al. [15–17] have used the hadronic model. In this model, Fermi-accelerated high energy protons interact with the SSC photons in the core region of the jet (few times the Schwarzschild radius R_S) to produce the Δ -resonance. Subsequently the Δ -resonance decays to charged and neutral pions as follows,

$$p + \gamma \rightarrow \Delta^+ \rightarrow \begin{cases} p \pi^0, \\ n \pi^+ \rightarrow n e^+ \nu_e \nu_\mu \bar{\nu}_\mu \end{cases} \quad (1)$$

The decay of neutral pions to TeV photons give the multi-TeV SED. The relationship between the π^0 -decay TeV photon energy E_γ and the target SSC photon energy ϵ_γ in the observer frame is given by

$$E_\gamma \epsilon_\gamma \simeq 0.032 \frac{\mathcal{D}^2}{(1+z)^2} \text{ GeV}^2, \quad (2)$$

where \mathcal{D} is the Doppler factor and z is the redshift. The observed TeV γ -ray energy and the proton energy E_p are related through

$$E_p = \frac{10\Gamma}{\mathcal{D}} E_\gamma, \quad (3)$$

where Γ is the bulk Lorentz factor of the relativistic jet. From Eqs. (2) and (3) it is observed that high energy protons collide with low energy SSC photons and vice versa to produce high energy γ -rays.

Multi-TeV emission is observed from many blazars and FR I galaxies by Cherenkov telescope arrays. These emission are classified into non-flaring and flaring events. For the non-flaring events (e.g. emission from Cen A[1]), the injected proton spectrum is a power-law given by $dN_p/dE_p \propto E_p^{-\alpha}$ with $\alpha \geq 2$. These protons will interact with the background SSC photons having comoving number density n'_γ (henceforth ' implies jet comoving frame) and satisfying the kinematical conditions in Eqs.(2) and (3). As discussed in ref.[17], the flaring occurs within a compact and confined volume of a smaller cone which is enclosed in a bigger cone as shown in Fig. 1 of ref.[17]. In this case the injected proton spectrum is a power-law with an exponential decay. In a unified manner we can express the injected proton spectrum for both non-flaring and flaring processes as[17, 21]

$$\frac{dN_p}{dE_p} \propto E_p^{-\alpha} \begin{cases} 1, & \text{non-flaring} \\ e^{-E_p/E_{p,c}}, & \text{flaring} \end{cases}, \quad (4)$$

where $E_{p,c}$ is the break energy for the high energy protons and above this break energy the proton spectrum falls very fast. These protons will interact in the flaring region having the comoving photon number density $n'_{\gamma,f}$ to produce the Δ -resonance. The density of the photons in the flaring region is much higher than the rest of the blob (non-flaring n'_γ) probably due to the copious annihilation of electron positron pairs, splitting of photons in the magnetic field and enhanced IC photons in this region. Here we observe that the spectrum has a exponential decay above the $E_{p,c}$ only for the flaring case. In this model the inner compact region has a radius R'_f smaller than the outer region radius R'_b i.e. $R'_f < R'_b$. We do not know exactly the properties of the inner jet except that the photon energy density is high compared to the outer one and the optical depth of the Δ -resonance process in this region is given by

$$\tau_{p\gamma} = n'_{\gamma,f} \sigma_{\Delta} R'_f. \quad (5)$$

The efficiency of the $p\gamma$ process depends on the physical conditions of the interaction region, such as the size, distance from the base of the jet, photon density and their distribution in the region. From Eq.(5) we can estimate the photon density in this region. On the other hand, the photon density in the outer region can be calculated from the observed flux. So, for this reason the scaling behavior of the photon densities in flaring and non-flaring region is assumed and is given by

$$\frac{n'_{\gamma,f}(\epsilon_{\gamma_1})}{n'_{\gamma,f}(\epsilon_{\gamma_2})} = \frac{n'_\gamma(\epsilon_{\gamma_1})}{n'_\gamma(\epsilon_{\gamma_2})}, \quad (6)$$

which implies that, the ratio of photon densities at two different background energies ϵ_{γ_1} and ϵ_{γ_2} in flaring and

non-flaring states remains the same. Previously we have used this assumption to explain successfully the flaring of the blazar 1ES1959+650 and the radio galaxy M87. Also, the number of π^0 -decay photons at a given energy is proportional to both the number of high energy protons and the density of the SSC background photons in the jet, i.e. $N(E_\gamma) \propto N(E_p)n'_\gamma$. For the flaring case n'_γ is replaced by the photon density in the flaring region given by $n'_{\gamma,f}$. The γ -ray flux from the π^0 decay is then given by

$$F_\gamma(E_\gamma) \equiv E_\gamma^2 \frac{dN(E_\gamma)}{dE_\gamma} \propto E_p^2 \frac{dN(E_p)}{dE_p} n'_{\gamma,f}. \quad (7)$$

Using the scaling behavior of Eq.(6), the observed multi-TeV photon flux from π^0 -decay at two different observed photon energies E_{γ_1} and E_{γ_2} can be expressed as

$$\frac{F_\gamma(E_{\gamma_1})}{F_\gamma(E_{\gamma_2})} = \frac{n'_\gamma(\epsilon_{\gamma_1})}{n'_\gamma(\epsilon_{\gamma_2})} \left(\frac{E_{\gamma_1}}{E_{\gamma_2}} \right)^{-\alpha+2} e^{-(E_{\gamma_1}-E_{\gamma_2})/E_c}, \quad (8)$$

where $E_{\gamma_{1,2}}$ correspond to the proton energy $E_{p_{1,2}}$ and we have used the relations $E_{p_1}/E_{p_2} = E_{\gamma_1}/E_{\gamma_2}$, and $E_{p_{1,2}}/E_{p,c} = E_{\gamma_{1,2}}/E_c$. By taking the ratio we get rid of the proportionality constant. By using the known flux at a particular energy in the flaring/non-flaring state, we can calculate the flux at other energies using Eq.(8) and also the normalization constant can be calculated.

In terms of SSC photon energy and its luminosity, the photon number density n'_γ is expressed as

$$n'_\gamma(\epsilon_\gamma) = \eta \frac{L_{\gamma,SSC}(1+z)}{\mathcal{D}^{2+\kappa} 4\pi R_b'^2 \epsilon_\gamma}, \quad (9)$$

where $\eta \sim 1$ is the efficiency of SSC process and $\kappa \sim (0-1)$ depending on whether the jet is continuous or discrete. In this work we consider $\kappa = 0$. The SSC photon luminosity is expressed in terms of observed flux ($\Phi_{SSC}(\epsilon_\gamma) = \epsilon_\gamma^2 dN_\gamma/d\epsilon_\gamma$) which is given by

$$L_{\gamma,SSC} = \frac{4\pi d_L^2 \Phi_{SSC}(\epsilon_\gamma)}{(1+z)^2}. \quad (10)$$

Furthermore, using Eq.(2), we can further simplify the ratio photon densities of Eq.(6) to

$$\frac{n'_\gamma(\epsilon_{\gamma_1})}{n'_\gamma(\epsilon_{\gamma_2})} = \frac{\Phi(\epsilon_{\gamma_1}) E_{\gamma_1}}{\Phi(\epsilon_{\gamma_2}) E_{\gamma_2}}. \quad (11)$$

Now we can express Eq.(8) in terms of observed SSC flux and E_γ as,

$$\frac{F_\gamma(E_{\gamma_1})}{F_\gamma(E_{\gamma_2})} = \frac{\Phi_{SSC}(\epsilon_{\gamma_1})}{\Phi_{SSC}(\epsilon_{\gamma_2})} \left(\frac{E_{\gamma_1}}{E_{\gamma_2}} \right)^{-\alpha+3} e^{-(E_{\gamma_1}-E_{\gamma_2})/E_c}. \quad (12)$$

Although Eqs.(8) and (12) give the same result, the latter form is much more simpler than the former one. Because the latter one simply uses the SED of SSC photon calculated using the leptonic model and does not calculate

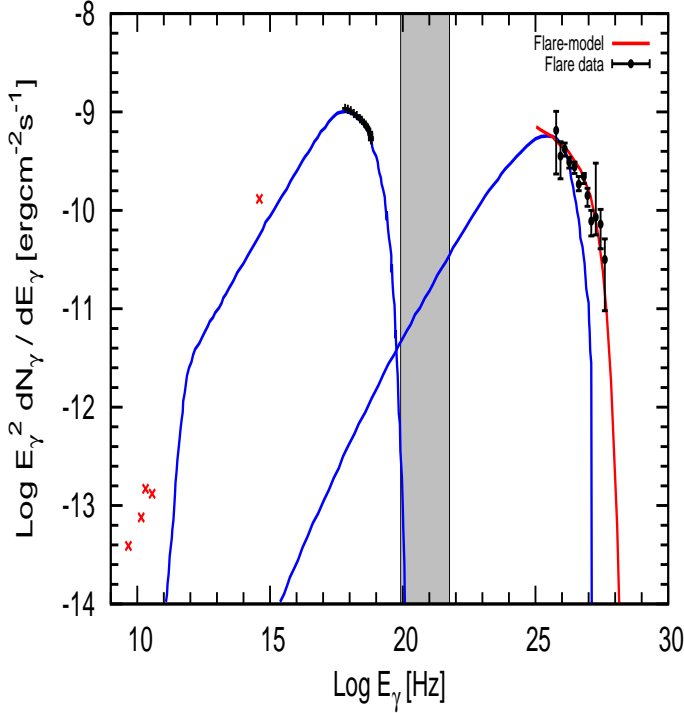


FIG. 1. The SED of Mrk 421 is shown in all the energy bands. The flare of April 2004 in multi-TeV energy is shown here. The hadronic model fit to the April 2004 data is shown as continuous line to the extreme right. The shaded region is the energy range of SSC photons where the Fermi-accelerated protons are collided to produce the Δ -resonance.

the photon densities at different energies which depend on the size of the emission region. Apart from that in the latter case we find the multi-TeV flux is proportional to $E_\gamma^{-\alpha+3}$ and $\Phi_{SSC}(\epsilon_\gamma)$ while in the former case it is proportional to $E_\gamma^{-\alpha+2}$ and the photon number density $n'_\gamma(\epsilon_\gamma)$. Finally we would like to point out that in the photohadronic process ($p\gamma$), the multi-TeV photon flux can be shown to be

$$F(E_\gamma) = A_\gamma \Phi_{SSC}(\epsilon_\gamma) \left(\frac{E_\gamma}{\text{TeV}} \right)^{-\alpha+3} e^{-E_\gamma/E_c}, \quad (13)$$

where A_γ is a dimensionless constant and both ϵ_γ and E_γ satisfy the condition given in Eq.(2). This formula will be used to calculate the multi-TeV flux from both non-flaring (without exponential decay term) and flaring events from AGN and their subclass if the emission is due to photohadronic process from the core region. For different blazars/AGN, the value of A_γ will be different which we shall discuss in the next section. We can calculate the Fermi accelerated high energy proton flux F_p from the TeV γ -ray flux through the relation

$$F_p(E_p) = 7.5 \times \frac{F_\gamma(E_\gamma)}{\tau_{p\gamma}(E_p)}. \quad (14)$$

The optical depth $\tau_{p\gamma}$ is given in Eq.(5).

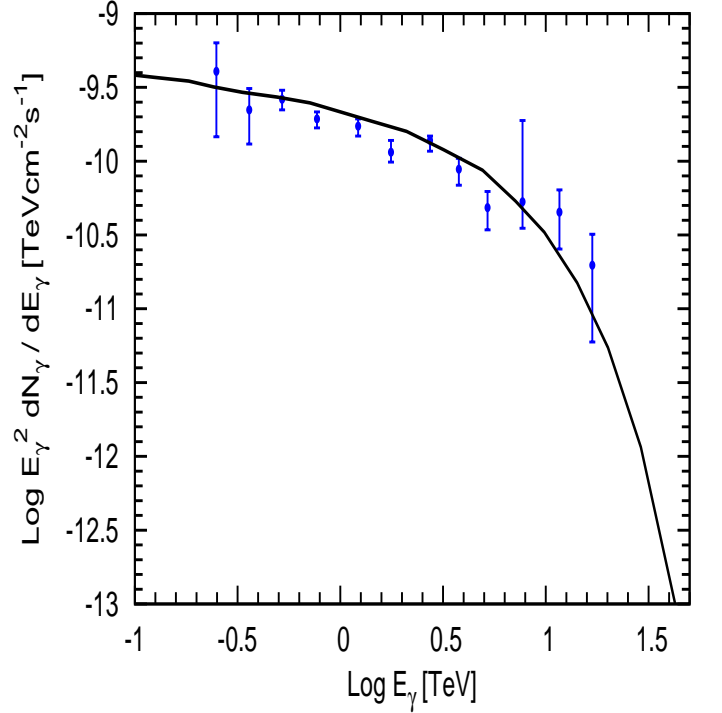


FIG. 2. The continuous curve is the hadronic model fit to the multi-TeV flaring data of Mrk 421.

III. MRK 421

Mrk 421 is a high synchrotron peaked BL Lac object (HBL) and is the first extragalactic source with a redshift of $z=0.031$ to be established as a TeV emitter[19]. It has a luminosity distance d_L of about 129.8 Mpc. Its central supermassive black hole has a mass $M_{BH} \simeq (2-9) \times 10^8 M_\odot$ corresponding to a Schwarzschild radius of $(0.6-2.7) \times 10^{14}$ cm and the Eddington luminosity $L_{Edd} = (2.5-11.3) \times 10^{46} \text{ erg s}^{-1}$. The synchrotron peak of its SED is in soft to medium x-ray range and the SSC peak is in the GeV range. It is one of the fastest varying γ -ray sources. In the past through dedicated multi wavelength observations, the source has been studied intensively. These studies show a correlation between x-rays and very high energy (VHE) γ -rays. A one-zone SSC model explains the observed SED reasonably well[20]. During April 2004, the source was flaring in x-rays as well as in γ -rays (TeV energy) regions. The source was observed simultaneously at TeV energies with the Whipple 10 m telescope and at x-ray energies with the Rossi x-ray Timing Explorer (RXTE). It was also observed simultaneously in radio and optical wavelengths. During the flaring it was observed that, the TeV flares had no coincident counterparts at longer wavelengths. Also it was observed that the x-ray flux reached its peak 1.5 days before the TeV flux did during this outburst. So it is believed that, the TeV flare might not be a true orphan flare like the one observed in 1ES 1959+650. On the other hand remarkable similarities between the orphan TeV flare in 1ES 1959+650 and Mrk 421 were observed,

including similar variation patterns in x-rays.

By using the one-zone SSC model, the average SED of Mrk 421 is fitted in Fig. 11 of ref. [11]. In this model, the spherical blob of size $R'_b \sim 0.7 \times 10^{16} \text{ cm}$ moves down the conical jet with a Lorentz factor $\Gamma \simeq 14$ and a Doppler factor of $\mathcal{D} = 14$. The emitting region is filled with an isotropic electron population and a randomly oriented magnetic field $B' = 0.26 \text{ G}$. In the present work we study the flaring of Mrk 421 during April 2004 by considering the particulars of the hadronic model as discussed above and use its corresponding parameters.

IV. RESULTS

The flaring of Mrk 421 in April 2004 was observed in the energy range $0.25 \text{ TeV} (6.0 \times 10^{25} \text{ Hz}) \leq E_\gamma \leq 16.85 \text{ TeV} (4.1 \times 10^{27} \text{ Hz})$ by Whipple telescope. In the hadronic model discussed above, this corresponds to the Fermi accelerated proton energy in the range $2.5 \text{ TeV} \leq E_p \leq 168 \text{ TeV}$ and the corresponding background photon energy will lie in the range $23.6 \text{ MeV} (5.7 \times 10^{21} \text{ Hz}) \geq \epsilon_\gamma \geq 0.35 \text{ MeV} (8.4 \times 10^{19} \text{ Hz})$. As can be observed from the shaded region of the Fig. 1, this range of ϵ_γ is in the low energy tail of the SSC photons. It is important to note that, in the orphan flaring of 1ES 1959+650 the ϵ_γ is also exactly in the low energy tail of the SSC photons[17], whereas for M87 flaring, it is in the rising part of the SSC photons[16]. For the calculation of normalized multi-TeV flux we take into account one of the observed TeV fluxes from the flare with its corresponding energy and with the use of Eq.(12) calculate other TeV fluxes. In this model the free parameters are the spectral index α and the TeV γ -ray cut-off energy E_c which are adjusted to obtain the best fit. Here we obtain the best fit for $\alpha = 2.713$ and $E_c = 6.16 \text{ TeV}$. This corresponds to the proton cut-off energy $E_{p,c} = 62 \text{ TeV}$. In Fig. 2 we have shown the fitting to the TeV flaring data only, which fits very well. In our results, the presence of $\Phi_{SSC}(\epsilon_\gamma)$ in Eq. (13) modifies the power-law with exponential fall scenario. From the best fit parameters we obtain the value of the dimensionless constant $A_\gamma \simeq 20$ in Eq. (13). By using the best fit parameters, we have also calculated the value of A_γ from the multi-TeV flare of 1ES 1959+650 and M87 and the multi-TeV emission from Centaurus A, which are given as 86, 1.86 and 8.6×10^{-4} respectively. We observe that for orphan flaring the condition $A_\gamma \gg 1$ is satisfied as is seen from 1ES 1959+650 and Mrk421. On the other hand for non-orphan flaring this value is small $A_\gamma \lesssim 1$.

In the flaring state, the proton luminosity L_p for the highest observed proton energy $E_p = 168 \text{ TeV}$ has to be smaller than the $L_{Edd} \sim 2.5 \times 10^{46} \text{ erg s}^{-1}$ and this gives $\tau_{p\gamma} \gtrsim 0.02$ in the inner jet region. For our estimate we consider the hidden jet size $R'_f \simeq 3 \times 10^{15} \text{ cm}$ which is in between R_s and the blob radius R'_b . Also in this region the maximum proton energy will be $E_{p,max} \sim 10^{18} (B'_f/1\text{G}) \text{ eV}$ and for larger magnetic field the $E_{p,max}$ can even be more as larger magnetic field is expected

within the hidden jet. In this region we obtain $n'_{\gamma,f} \gtrsim 1.3 \times 10^{10} \text{ cm}^{-3}$, which shows that the photon density in this region is really very high.

These high energy protons will be accompanied by high energy electrons in the same energy range. In the magnetic field of the jet, these electrons will emit synchrotron photons in the energy range $4 \times 10^{19} \text{ Hz}$ to $2 \times 10^{23} \text{ Hz}$, which is in the lower part of the SSC spectrum and will not be observable because of the lower flux. Similarly the multi-TeV photons in the energy range $0.25 \text{ TeV} \lesssim E_\gamma \lesssim 16.85 \text{ TeV}$ can interact with the background photons to produce e^+e^- pair and these individual electron or positron will have energy $E_\gamma/2$. Also the positron produced from the π^+ decay will have energy $E_\gamma/2$. These e^- and e^+ will radiate synchrotron photons in the energy range $2 \times 10^{17} \text{ Hz}$ to $9 \times 10^{20} \text{ Hz}$. The flux $F_{e^+,syn}$ from the synchrotron radiation of e^+ produced from the π^+ decay will be $F_{e^+,syn} \ll 8 \times 10^{-11} \text{ erg cm}^{-2} \text{ s}^{-1}$. The mean free path satisfies the constraint $\lambda_{\gamma\gamma} = (n'_{\gamma,f} \sigma_{\gamma\gamma})^{-1} \gg R'_f$ so hardly any multi-TeV photons will interact with the background photons to produce e^+e^- pair in the inner jet region. From the above analysis we observe that, the photon fluxes from the synchrotron emission of the electrons and positrons are not observable during the flaring event of Mark 421 in April 2004, which makes this flare orphan like the one observed in 1ES 1959+650. In principle, the multi-TeV flux from Mrk 421 can be reduced due to the absorption of TeV photons by the diffuse extragalactic background radiation through the process $\gamma_{\text{TeV}} + \gamma_b \rightarrow e^+e^-$. But the energy range of our interest is $.25 \text{ TeV} \leq E_\gamma \leq 17 \text{ TeV}$ and at this energy range, the spectral shape remains nearly unchanged due to the almost constant optical depth for most of the extragalactic background radiation[21].

From the study of the flaring events in blazars, we observe that the flaring phenomena can be explained through the photohadronic interaction in a compact and confined region within the blazar jet where the photon density is high and this region is near to the nuclear region. As observed, flaring can occur in any blazar. But from the study of 1ES 1959+650 and Mrk 421, we deduce that orphan flaring can only be possible for those blazars which have a deep valley in between the end of the synchrotron SED and the beginning of the SSC SED as shown in Fig. 1. We note that the HBLs Mrk 501 and PG 1553+113 are probable candidates for orphan flaring in future. For the orphan flaring events we find $A_\gamma \gg 1$ and for non-orphan flaring $A_\gamma \lesssim 1$.

If Mrk 501 were to produce an orphan flare then the flare energy will lie in the range $1 \text{ TeV} \lesssim E_\gamma \lesssim 8.6 \text{ TeV}$ and this corresponds to the background SSC photon energy in the range $4.3 \text{ MeV} \gtrsim \epsilon_\gamma \gtrsim 0.5 \text{ MeV}$. We estimate this by taking the parameters of Mrk 501 as follows: $\mathcal{D} = 12$, $z = 0.031$ from ref.[22]. In this case the maximum Fermi-accelerated proton energy will be $E_p \leq 10 E_\gamma \sim 86 \text{ TeV}$. Also, another condition which

must hold for the orphan flaring is

$$A_\gamma = \frac{F(8.6 \text{ TeV})}{\Phi_{SSC}(0.5 \text{ MeV})} \left(\frac{1}{8.6} \right)^{-\alpha+3} e^{8.6/(E_c/\text{TeV})} \gg 1. \quad (15)$$

One has to remember that, if \mathcal{D} changes, accordingly the values of E_γ , ϵ_γ and the E_p will also change.

V. CONCLUSIONS

The orphan flaring of Mrk 421 can be explained well by the hadronic model. We observe that, in this model, the multi-TeV photon flux is proportional to $\Phi_{SSC}(\epsilon_\gamma)$, $E_\gamma^{-\alpha+3}$ and an exponential decay term as shown in Eq.

(13). This implies that, the Fermi accelerated protons interact with the background photons (in the low energy tail) of the SSC spectrum. During the April 2004 flaring of Mrk 421, we have shown that the flux from the synchrotron emission from the high energy e^+ and e^- is suppressed compared to the normal flux implying that the flaring was orphan in nature, like the one observed in 1ES 1959+650. We have also shown what type of blazar spectrum will give orphan flaring and predict that Mrk 501 and PG 1553+113 are possible candidates for orphan flaring in future.

ACKNOWLEDGMENTS

The work of S.S. is partially supported by DGAPA-UNAM (Mexico) Project No. IN110815.

-
- [1] A. A. Abdo *et al.* [Fermi LAT Collaboration], *Astrophys. J.* **719**, 1433-1444 (2010). [arXiv:1006.5463 [astro-ph.HE]].
 - [2] P. Roustazadeh and M. Böttcher, *Astrophys. J.* **728**, 134 (2011).
 - [3] G. Fossati, L. Maraschi, A. Celotti, A. Comastri and G. Ghisellini, *Mon. Not. Roy. Astron. Soc.* **299** (1998) 433 [arXiv:astro-ph/9804103].
 - [4] G. Ghisellini, A. Celotti, G. Fossati, L. Maraschi and A. Comastri, *Mon. Not. Roy. Astron. Soc.* **301** (1998) 451 [arXiv:astro-ph/9807317].
 - [5] C. D. Dermer and R. Schlickeiser, *Astrophys. J.* **416**, 458 (1993).
 - [6] M. Sikora, M. C. Begelman and M. J. Rees, *Astrophys. J.* **421**, 153 (1994).
 - [7] F. Aharonian *et al.* [HESS Collaboration], *Astrophys. J.* **695**, L40 (2009) [arXiv:0903.1582 [astro-ph.CO]].
 - [8] A. Abramowski *et al.* [H.E.S.S. and VERITAS Collaborations], *Astrophys. J.* **746**, 151 (2012) [arXiv:1111.5341 [astro-ph.CO]].
 - [9] H. Krawczynski, S. B. Hughes, D. Horan, F. Aharonian, M. F. Aller, H. Aller, P. Boltwood and J. Buckley *et al.*, *Astrophys. J.* **601**, 151 (2004) [astro-ph/0310158].
 - [10] W. Cui *et al.* [VERITAS Collaboration], *AIP Conf. Proc.* **745**, 455 (2005) [astro-ph/0410160].
 - [11] M. Blazewski, G. Blaylock, I. H. Bond, S. M. Bradbury, J. H. Buckley, D. A. Carter-Lewis, O. Celik and P. Cogan *et al.*, *Astrophys. J.* **630**, 130 (2005) [astro-ph/0505325].
 - [12] A. Atoyan and C. D. Dermer, *Phys. Rev. Lett.* **87**, 221102 (2001) [astro-ph/0108053].
 - [13] A. M. Atoyan and C. D. Dermer, *Astrophys. J.* **586**, 79 (2003) [astro-ph/0209231].
 - [14] C. D. Dermer, K. Murase and H. Takami, *Astrophys. J.* **755**, 147 (2012) [arXiv:1203.6544 [astro-ph.HE]].
 - [15] S. Sahu, B. Zhang and N. Fraija, *Phys. Rev. D* **85**, 043012 (2012) [arXiv:1201.4191 [astro-ph.HE]].
 - [16] S. Sahu and E. Palacios, arXiv:1310.1381 [astro-ph.HE].
 - [17] S. Sahu, A. F. O. Oliveros and J. C. Sanabria, *Phys. Rev. D* **87**, 103015 (2013) [arXiv:1305.4985 [hep-ph]].
 - [18] F. Aharonian *et al.* [HEGRA Collaboration], *Astron. Astrophys.* **406**, L9 (2003) [astro-ph/0305275].
 - [19] M. Punch, C. W. Akerlof, M. F. Cawley, M. Chantell, D. J. Fegan, S. Fennell, J. A. Gaidos and J. Hagan *et al.*, *Nature* **358**, 477 (1992).
 - [20] A. A. Abdo *et al.* [MAGIC Collaboration], *Astrophys. J.* **736**, 131 (2011).
 - [21] F. Aharonian *et al.* [HEGRA Collaboration], *Astron. Astrophys.* **406**, L9 (2003) [astro-ph/0305275].
 - [22] B. Bartoli *et al.* [ARGO-YBJ Collaboration], *Astrophys. J.* **758**, 2 (2012) [arXiv:1209.0534 [astro-ph.HE]].